Journal of
Nanoelectronics and Optoelectronics
Vol. 2, 1–7, 2007

REVIEW

Inter-Valence-Band Hot Hole Laser in Two-Dimensional Delta-Doped Homoepitaxial Semiconductor Structures

R. E. Peale*, M. V. Dolguikh, and A. V. Muravjov

Department of Physics and College of Optics and Photonics, University of Central Florida, Orlando, FL 32816, USA

This paper reviews, compares, and contrasts recent gain calculations for a laser concept in delta-doped p-Ge and p-GaAs. Gain is calculated using distribution functions, determined from Monte Carlo simulations, for hot holes in crossed electric and magnetic fields. The results suggest that Ge is the superior material when considering only the factor of optical gain, but the possibility of lasing in GaAs can take advantage of a wider range of growth opportunities.

Keywords: Terahertz, Far-Infrared, Laser, Germanium, Gallium Arsenide.

The under-utilized THz region of the electromagnetic spectrum has been of recent interest for a variety of applications. For purposes of discussion, we focus on defense applications, where the THz spectrum can be divided informally into three regimes. The "low-THz" below about 1 THz would be useful for seeing in dusty "brown-out" conditions, e.g., in helicopter landings. In this region, there is less scattering by dust particles than in the IR, better spatial resolution than possible using mm-waves, and significantly less atmospheric water vapor attenuation than in the "mid-" and "upper-THz," corresponding to the ranges 1–4 and 4–10 THz, respectively. These latter regions have their own proposed applications, namely advanced threat warning systems, remote earth sensing, and flame/plasma characterization. The division of the spectrum above 1 THz by the present authors into the ranges specified is based on purely technological considerations: Semiconductor lasers made from bulk p-Ge[1] and GaAs–AlGaAs quantum wells[2] are known in the 1–4 THz region, while no semiconductor lasers are known in the 4–10 THz range.

The authors have worked for many years to advance the technology of inter-valence-band hot hole lasers based on bulk rods of p-Ge having ∼cubic centimeter active volume.[3–19] One of us (AVM) has been involved in this research since its beginnings more than two decades ago.[20] Features of this laser are broad tunability (1.5–4.2 THz) with high spectral density in a single device (Fig. 1) and high >1 W peak power. Disadvantages are a low duty ($1\ \mu s \times 10$ Hz) and low temperature ($T < 15$ K) operation. Until recently, the p-Ge laser was the only far-infrared semiconductor laser known. The first commercial sale of a complete p-Ge laser system occurred in 2006.[21]

Recently quantum cascade lasers (QCL) have emerged in the mid-THz wavelength region.[2] These feature continuous wave operation at temperatures above 80 K, and consequently, compared with p-Ge lasers, QCLs have been rather quickly adopted for consideration in various THz applications. QCLs are not without their own drawbacks, however. The wavelength of a single device is essentially fixed with only a small range of temperature tuning possible. Their output power is low, of order ∼mW. To obtain the highest useful power one naturally wishes to operate at the lowest possible temperatures. High precision molecular beam epitaxy is required for their production, which has resulted in high price per individual laser chip.[24]

A recent goal of our research has been to consider new hot-hole laser concepts that might combine the features and eliminate the disadvantages of both existing laser systems. To appreciate these concepts, it is first necessary to review the basic inter-valence-band mechanism, which is presented in Figure 2 for any cubic semiconductor. In Figure 2, one sees that an inversion population of light-holes builds up for certain ratios of electric and magnetic fields. The pumping of the upper laser level relies on optical phonon scattering, and in Figure 2 both polar and non-polar flavors are indicated, together with the energy threshold for them to occur. Polar optical phonon scattering occurs only in polar semiconductors, such as GaAs, and its defining feature is a high probability that results in a "hard ceiling" at the energy threshold. Such behavior

*Author to whom correspondence should be addressed.

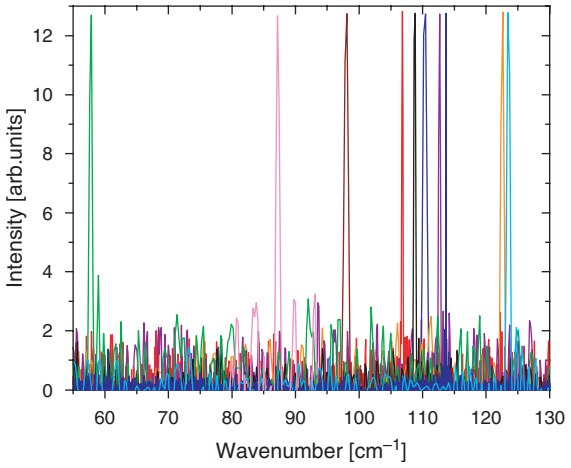

Fig. 1. Superposition of ten separate single-line emission spectra obtained from a p-Ge laser using intracavity wavelength selectors (after Ref. [22]). These data were collected using a Bomem DA8 Fourier spectrometer with highest resolution 0.02 cm^{-1}, using an event-locking accessory[23] for pulsed sources.

is in contrast to non-polar optical phonon scattering, which allows penetration of holes to energy regions significantly above the optical phonon scattering threshold.

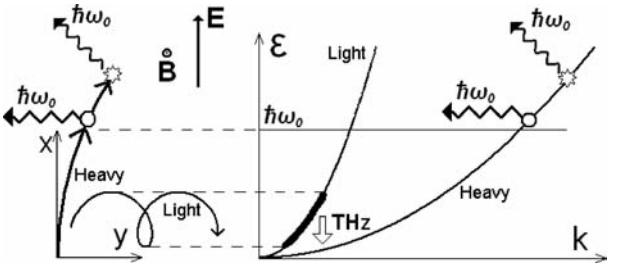

Fig. 2. Mechanism of intersubband population inversion and far-infrared gain for cubic semiconductors in crossed electric and magnetic fields. The left part of the diagram shows light and heavy hole trajectories in coordinate space. The right part of the diagram shows light- and heavy-hole subband energies versus momentum wavevector together with trajectories and vertical inter-valence-band radiative transitions. The optical phonon scattering threshold is indicated by the horizontal line $\hbar\omega_0$ in both parts. Non-polar optical phonon emission by heavy holes is indicated by wavy arrows, and polar optical phonon scattering is indicated by zig–zag arrows.

It is obvious from Figure 2 that any factor that decreases the light hole life time will also decrease the gain on terahertz optical transitions. Such factors include scattering of hot holes by ionized impurities, by other holes, and by acoustic phonons, since these all disrupt the required

R. E. Peale is a Professor of Physics at the University of Central Florida. He received a BA in Physics from UC Berkeley in 1983 and a Ph.D. in Physics at Cornell in 1990. After a postdoc at Lehigh University, he joined the UCF faculty in 1991.

M. V. Dolguikh received the BS and MS degrees from the Moscow Institute of Physics & Technology, and he received a Ph.D. in Physics from UCF in 2005. He is currently a research scientist with CAD Sciences, Inc. in White Plains, NY.

A. V. Muravjov is a Research Scientist at the Institute for Physics of Microstructures, Russian Academy of Science, Nizhny Novgorod, where he has been a member of the research team that invented p-Ge lasers since the early 1980s. He has been a Visiting Scientist at UCF since 1997.

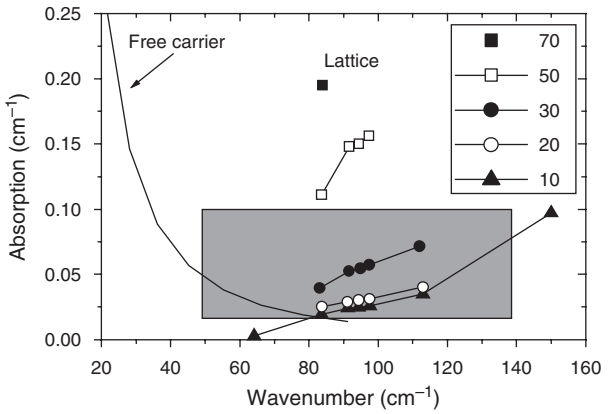

Fig. 3. Far-infrared absorption in Ge. Temperature dependent lattice absorption from Ref. [25] is plotted as connected symbols, with temperature in K indicated in the legend. Free carrier absorption for hole concentration 2×10^{14} cm^{-3} calculated for typical bulk p-Ge distribution functions is plotted as a solid curve. The horizontal borders of the shaded box are the range of reported gain values for p-Ge, with the vertical borders correspond to the maximum tuning range.

anisotropic hole momentum distribution. In practice, the inter-valence-band lasing mechanism has been observed experimentally only in p-Ge.

It is also obvious that any absorption in the crystal at THz frequencies will lower the net gain. Such absorption is present due to free carriers and thermally excited acoustic phonons. Figure 3 presents the temperature-dependent absorption spectrum for Ge, and when compared to the range of reported gain values for p-Ge lasers (shaded box in Fig. 3), these data explain both the observed tuning limitations of the p-Ge laser and its maximum temperature of operation. The only way to increase wavelength range and operating temperature is to substantially increase the gain.

Opportunities for increasing the gain are limited in p-Ge. We have focused on remediating of one of the effects that decrease the light-hole lifetime, namely ionized impurity scattering. Figure 4 explains clearly the importance of impurity scattering on the gain.[26] While the gain g is proportional to the number of holes N, the gain

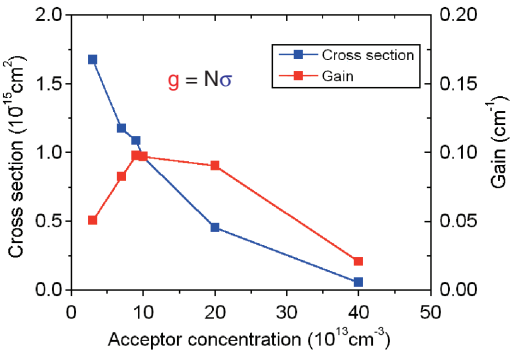

Fig. 4. Gain cross section as a function of acceptor cross-section as determined from Monte-Carlo simulated hot-hole distribution functions.[26] Gain is the product of cross section and hole concentration. The maximum gain occurs near 10^{14} cm^{-3}.

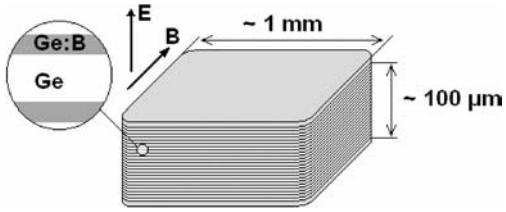

Fig. 5. Delta-doped Ge laser structure.

is also proportional to the gain cross section σ, which decreases strongly with increasing acceptor concentration due to scattering of light holes on the ionized impurity centers. Consequently, the optimum net gain is calculated to occur at rather low acceptor concentrations of $\sim 10^{14}$ cm^{-3}, which agrees very well with experimental observations.

Our approach to increasing light-hole lifetime is to reduce the effects of ionized impurity scattering by spatially separating the acceptor impurities from the light-hole accumulation regions in the crystal. The concept that we explored theoretically is periodic delta doping, which is presented schematically in Figure 5. Regions of undoped semiconductor (Ge is shown in Fig. 5) that are thicker than the likely light-hole cyclotron orbit diameter (of order 100 nm) are grown between thinner layers of doped material, which provides the necessary holes. To minimize electrodynamic losses, in order to take best advantage of the achieved gain increases, it is necessary that the optical thickness be greater than the emission wavelength ($\sim$100 μm in free space). We anticipate that the physical thickness achievable in such a structure to be as much as 100 μm[17] for Ge grown by chemical vapor deposition, which is 4 times the operating wavelength within the active crystal. For GaAs grown by vapor phase epitaxy, the thickness might even approach 1 mm.[27]

In order to consider the effects of the Figure 5 design and the dependence of its performance on geometry, temperature, and doping, we calculate gain from hot-hole distribution functions simulated by the Monte-Carlo method.[17] In this method, we compute hole trajectories in crossed E and B fields while keeping track of hole energy, position, and the space-charge distribution. Scattering on acoustic phonons, optical phonons, ionized impurities, and other holes is accounted for using known formulas. For hole–hole interaction, we use formulas developed by us.[18] The simulation outputs are light and heavy hole distribution functions $f_{\mathrm{lh}}(k, r)$. Spatial and spectral optical gain profiles are then calculated from

$$\alpha(r, \nu) = p(r) \int_k z_{\mathrm{lh}}(k)[f_{\mathrm{l}}(k, r) - f_{\mathrm{h}}(k, r)] \times \delta(E_{\mathrm{l}}(k) - E_{\mathrm{h}}(k) - h\nu)\, d^3k \qquad (1)$$

where p is the hole concentration, z_{lh} is the oscillator strength, and k the momentum wavevector.

The simulation is performed on a personal computer. Figure 6 is an image from part of the screen window used

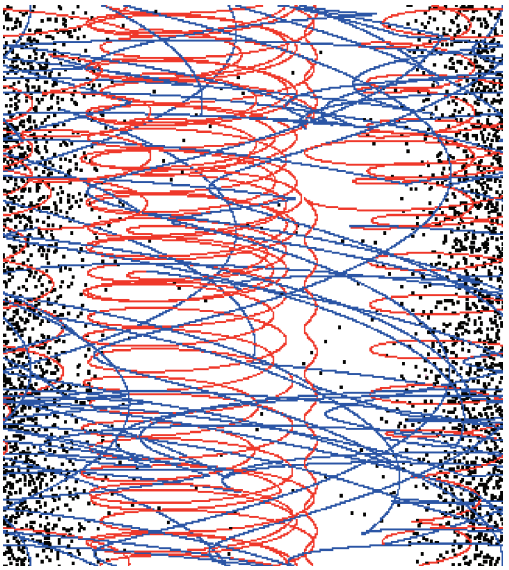

Fig. 6. Computer screen capture of Monte Carlo simulation.

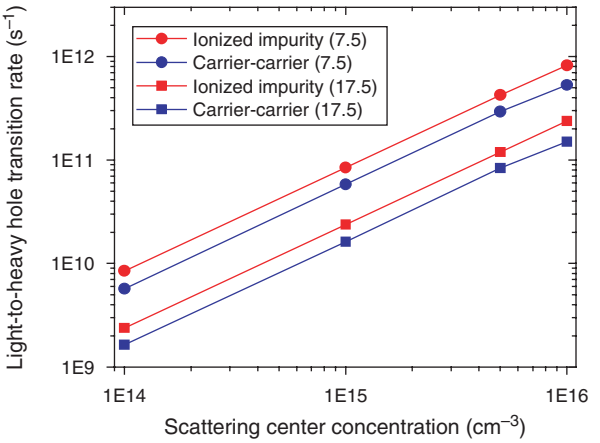

Fig. 7. Carrier–carrier and ionized impurity scattering rates for the light-to-heavy hole non-radiative intersubband transition averaged over typical p-Ge laser light- and heavy-hole distribution functions (E = 1.5 kV/cm, $B = 1.1$ T, $T = 10$ K) versus scattering center concentration. Values in the legend indicate initial light hole kinetic energy in meV. From Ref. [28].

to monitor the simulation progress. The black dots represent ionized impurities, and these are grouped into layers with a diffused spatial distribution according to the delta-doping profile that we explored. Blue curves are heavy hole trajectories, while the tighter red looping trajectories are those of light holes. The program keeps track of the spatial position of the simulated hole (which recursively enters the frame via periodic boundary conditions), its energy, and the scattering events that occur according to their probability. Also recorded is the percent of the time that the hole spends in the light hole band.

One can see from Figure 6 that light holes within the undoped region live for many cyclotron cycles without scattering. In contrast, heavy holes interact strongly with impurities during every cycle. Several impurity scattering events with large change in momentum can be seen in Figure 6. Also evident in Figure 6 are a few inter-valence-band transitions.

While the delta-doping is obviously successful in segregating the fixed ionized impurity centers, it is more difficult to corral the mobile heavy holes, which also contribute Coulomb scattering. Figure 6 shows considerable numbers of heavy holes crossing the undoped region. Hence it is necessary to consider carefully the effect of these holes on gain. We developed a physically meaningful model of hole–hole scattering,[18] which is more accurate than the approximations that had been used previously. Together with the Monte Carlo method, it was possible to compare accurately the effect of the different scattering centers (fixed ionized acceptors and mobile holes) on light hole lifetime. Figure 7 compares the inversion-decreasing light-to-heavy hole transitions caused by scattering on impurities or on other holes. At all energies and scattering center concentrations considered, the ionized impurities cause more scattering than the comparatively insubstantial holes. Thus, simply segregating the impurity centers can provide significant benefit. Where the heavy holes congregate is a lesser consideration.

Even though the effect of hole–hole scattering is less of a concern than impurity scattering, it remains as a negative factor. However, we find that despite casual appearances in Figure 5, the heavy holes tend to accumulate near the acceptor centers leaving the light holes relatively undisturbed in the undoped layers. Figure 8 presents the Monte-Carlo simulated distribution functions for light and heavy holes in delta-doped Ge.[17] It is clear that heavy holes tend to accumulate near the doped layers, while light holes congregate with long lifetimes in the undoped regions.

Figure 9 presents spatially averaged gain spectra calculated using Eq. (1) from distributions such as those in Figure 8 for a specific delta-doped germanium device.[17] By comparing with Figure 3, one sees that nearly a factor 10 increase over bulk p-Ge can be achieved in the maximum gain. As the applied fields increase, the gain increases, so that at the higher fields the gain exceeds the experimental lattice absorption at a temperature of 50 K. Even higher applied fields are expected to produce net gain at temperatures up to 77 K. However, the quasiclassical assumptions used in the Monte-Carlo simulation become somewhat questionable at these fields, so we withhold the results of those high field calculations.

We recently completed calculations on GaAs delta-doped structures.[27] Ge and GaAs have nearly the same optical phonon energy, but a critical difference between them is the polar optical phonon scattering in GaAs, which provides a "hard ceiling" for hot holes in this material. When holes emit optical phonons at energies close to the optical phonon threshold, they return very near to $k = 0$. Hence, in GaAs, holes tend to scatter back to lower energies than in Ge. Both hard ceiling and concentration at

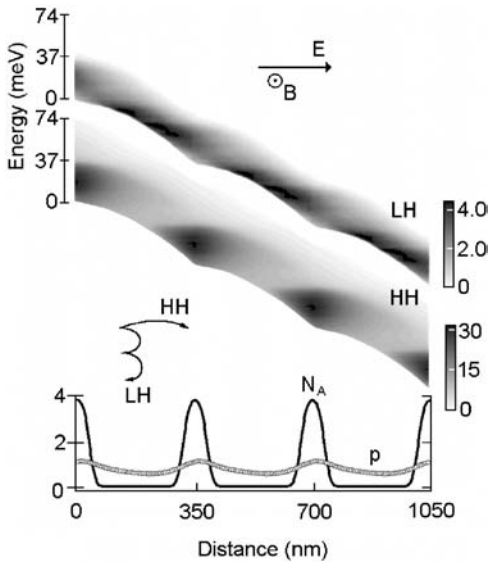

Fig. 8. Spatial separation of carriers and intersubband mechanism of THz amplification for delta-doped multilayer Ge structures in $E \times B$ fields. Dark areas represent high concentrations of light holes (upper band) and heavy holes (lower band). The shading scale is in units of 10^{12} cm^{-3} meV^{-1}. Spatial dependence of the zero-energy edge of the hole distribution reflects the self-consistent potential profile. Acceptor concentration profile N_A and total hole concentration p across the structure are plotted in units of 10^{15} cm^{-3}. Simulation parameters were $E = 1.5$ kV/cm, $B = 1.15$ T, $T = 10$ K, and $N_{av} = 8 \times 10^{14}$ cm^{-3}. Schematic light and heavy hole cyclotron trajectories are drawn to scale in coordinate space. From Ref. [17].

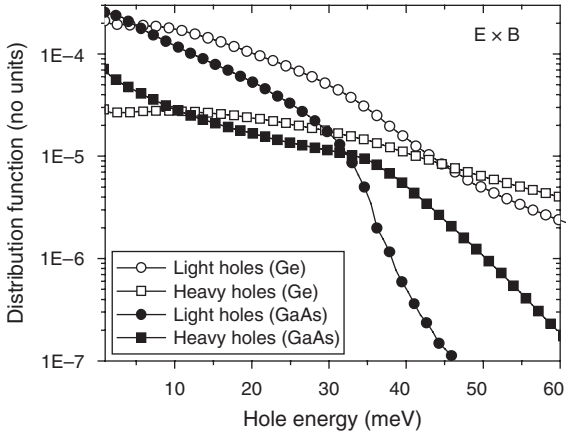

Fig. 10. Distribution functions of light and heavy holes in Ge and GaAs as a function of hole energy. The optical phonon scattering threshold is 37 and 35 meV, respectively. From Ref. [27].

low energies are revealed in the comparison of distribution functions for GaAs and Ge in Figure 10.

From the distribution functions alone, one might expect that the gain spectrum for GaAs would be shifted to lower THz frequencies than that of Ge. This might favor GaAs over Ge for the low-THz applications mentioned in the introduction. However, a negative factor of scattering to low energies is that holes in GaAs will be on average slower, and hence more subject to ionized impurity scattering. Compounding this effect is the smaller permittivity of GaAs, which results in weaker dielectric screening of the impurities. Additionally, any additional low frequency gain must struggle against rapidly increasing free-carrier absorption (Fig. 3), which turns out to be stronger in GaAs than in Ge (see below).

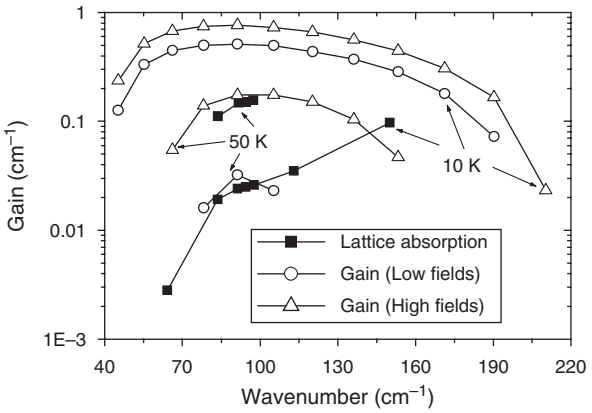

Fig. 9. Spatially-averaged calculated THz gain spectra (open symbols) with $N_{av} = 8 \times 10^{14}$ cm^{-3} for low ($E = 1.5$ kV/cm, $B = 1.15$ T) and high ($E = 2.5$ kV/cm, $B = 2$ T) applied fields at two different lattice temperatures. Experimental lattice absorption spectra[25] in Ge at $T = 10$ K and 50 K are plotted as solid symbols. From Ref. [17].

To consider the sum total of all effects, we first compare in Figure 11 the calculated gain spectra in bulk unstructured p-GaAs[27] and p-Ge.[29] The raw gain is indeed found to be larger for GaAs at low frequencies. At 50 cm^{-1}, it is more than double that of Ge. However, the calculated free carrier absorption is also larger for GaAs, and when it is subtracted, the resulting net gain for GaAs is lower than that of Ge at all frequencies. Moreover, the peak of gain curves for the two materials occurs at very similar wavenumbers, and there appears to be no low-frequency advantage for GaAs at all. The relatively small gain in bulk p-GaAs partially explains why inter-valence-band lasing has never been observed in this material, although the prediction of net positive gain (here, and in Ref. [30]) suggests that more (or even some) experimental effort is worthwhile simply to satisfy intellectual curiosity.

Because the technology for growing GaAs thin films is more developed than for Ge, it is very interesting to consider the improvements one might obtain by periodic delta doping of GaAs. Applying our calculations to this material results in the gain spectrum of Figure 12. Comparison with Figure 11 shows that gain improvement is significant, but at less than a factor of 2 this improvement is disappointing compared to the factor of ~10 found for Ge. This is partially explained by the comparatively severe effects of impurity scattering in GaAs, which limit the optimum carrier concentration in the structure to a value little more than that optimum for bulk.[27] (In Ge, the optimum concentration for the structure was 5 times higher than for bulk). Thus, the only advantage of GaAs over Ge might be technological, whereby certain growth techniques such

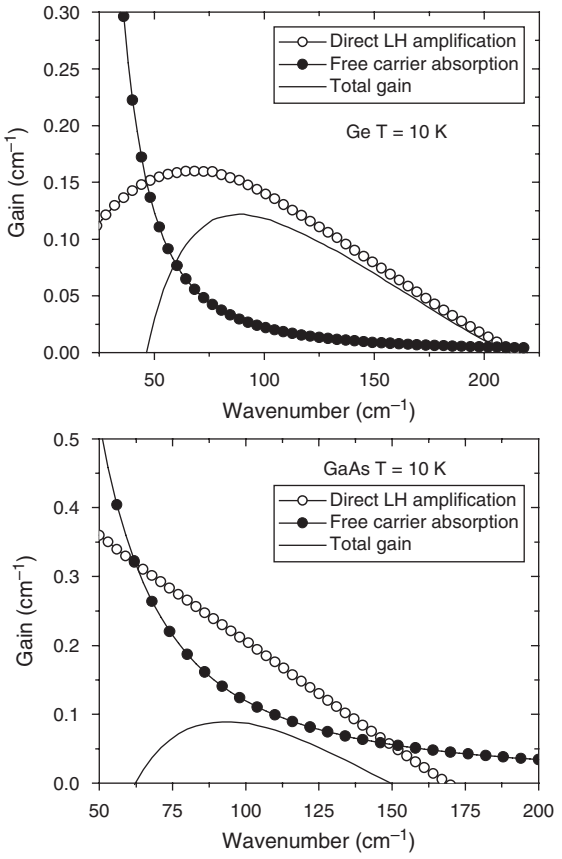

Fig. 11. Comparison of calculated spectra for raw gain, free carrier absorption, and net gain in bulk p-Ge (upper, from Ref. [29]) and p-GaAs (lower, from Ref. [27]). Losses due to absorption by acoustic phonons are not included.

as vapor phase epitaxy might produce remarkably thick, low-loss active media.

Compared with Ge, which can lase with applied magnetic fields as low as 0.35 T, GaAs requires rather strong fields to produce any gain at all. However, delta-doping provides some relief,[27] reducing for example the lasing threshold for a device with gain of 0.15 cm^{-1} from 5 T to 3 T.

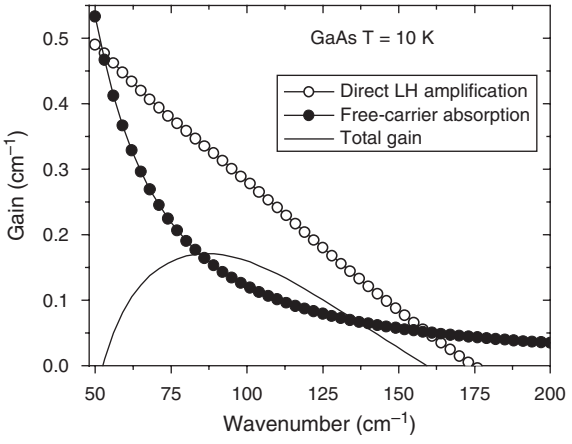

Fig. 12. Calculated gain spectrum for delta-doped GaAs.

In summary, gain calculations for periodically delta-doped homoepitaxial p-GaAs/GaAs THz laser structures have been compared to those of similar p-Ge/Ge laser structures. The GaAs structure gives lower gain and requires higher applied fields. On the other hand, GaAs has potentially better epitaxial growth opportunities. Experimental demonstration of the THz laser structure is needed for both materials. Besides providing closure to a question of intellectual interest, such experiments may provide a possible alternate to the QCL THz laser, but with the additional feature of a broad tuning range (24 THz) in a single device.

Acknowledgments: Monte Carlo simulations at UCF were initiated under subcontract from Zaubertek, Inc., who were funded by an AFOSR STTR award F49620-02-0025. The GaAs calculations were initiated during a ASEE/AFOSR Faculty Summer Fellowship in 2005 and subsequently supported by the Air Force Office of Scientific Research via a grant from AFRL/SNHC Hanscom AFB. We also acknowledge useful discussions with AFRL/SNHC Hanscom AFB staff scientists Walter Buchwald, Candace Lynch, David Bliss, David Weyburne, and Richard Soref.

References and Notes

1. E. Bründermann, Long Wavelength Infrared Semiconductor Lasers, edited by H. K. Choi, Wiley, NJ **(2004)**, pp. 279–343.
2. R. Kohler, A. Tredicucci, F. Beltram, H. E. Beere, E. H. Linfield, A. G. Davies, D. A. Ritchie, R. C. Iotti, and F. Rossi, *Nature* 417, 156 **(2002)**.
3. Kijun Park, R. E. Peale, H. Weidner, and J. J. Kim, Submillimeter p-Ge laser using a voigt-configured permanent magnet. *IEEE J. Quant. Electron.* 32, 1203 **(1996)**.
4. A. V. Muravjov, R. C. Strijbos, C. J. Fredricksen, H. Weidner, W. Trimble, S. H. Withers, S. G. Pavlov, V. N. Shastin, and R. E. Peale, *Appl. Phys. Lett.* 73, 3037 **(1998)**.
5. A. V. Muravjov, R. C. Strijbos, C. J. Fredricksen, S. H. Withers, W. Trimble, S. G. Pavlov, V. N. Shastin, and R. E. Peale, *Appl. Phys. Lett.* 74, 167 **(1999)**.
6. A. V. Muravjov, S. H. Withers, S. G. Pavlov, V. N. Shastin, and R. E. Peale, *J. Appl. Phys.* 86, 3512 **(1999)**.
7. A. V. Muravjov, S. H. Withers, R. C. Strijbos, S. G. Pavlov, V. N. Shastin, and R. E. Peale, *Appl. Phys. Lett.* 75, 2882 **(1999)**.
8. A. V. Muravjov, S. H. Withers, H. Weidner, R. C. Strijbos, S. G. Pavlov, V. N. Shastin, and R. E. Peale, *Appl. Phys. Lett.* 76, 1996 **(2000)**.
9. E. W. Nelson, A. V. Muravjov, S. G. Pavlov, V. N. Shastin, and R. E. Peale, *Infrared Physics and Technology* 42, 107 **(2001)**.
10. E. W. Nelson, S. H. Withers, A. V. Muravjov, R. C. Strijbos, R. E. Peale, S. G. Pavlov, V. N. Shastin, and C. J. Fredricksen, High-resolution study of composite cavity effects for p-Ge lasers. *IEEE J. Quant. Electron.* 37, 1525 **(2001)**.
11. A. V. Muravjov, E. W. Nelson, R. E. Peale, V. N. Shastin, and C. J. Fredricksen, *Infrared Physics & Technology* 44, 75 **(2003)**.
12. C. J. Fredricksen, E. W. Nelson, A. V. Muravjov, and R. E. Peale, *Infrared Physics and Technology* 44, 79 **(2003)**.
13. T. W. Du Bosq, R. E. Peale, E. W. Nelson, A. V. Muravjov, C. J. Fredricksen, N. Tache, and D. B. Tanner, *J. Appl. Phys.* 94, 5474 **(2003)**.

14. T. W. Du Bosq, R. E. Peale, E. W. Nelson, A. V. Muravjov, D. A. Walters, G. Subramanian, K. B. Sundaram, and C. J. Fredricksen, *Optics & Laser Technology* 37, 87 **(2005)**.
15. E. W. Nelson, M. V. Dolguikh, A. V. Muravjov, E. S. Flitsiyan, T. W. Du Bosq, R. E. Peale, S. H. Kleckley, C. J. Fredricksen, and W. G. Vernetson, *J. Appl. Phys.* 96, 1 **(2004)**.
16. T. W. Dubosq, A. V. Muravjov, R. E. Peale, and C. J. Fredricksen, *Appl. Opt.* 44, 7191 **(2005)**.
17. M. V. Dolguikh, A. V. Muravjov, R. E. Peale, M. Klimov, O. A. Kuznetsov, and E. A. Uskova, *J. Appl. Phys.* 98, 023107 **(2005)**.
18. M. V. Dolguikh, A. V. Muravjov, and R. E. Peale, *Phys. Rev. B* 73, 075327 **(2005)**.
19. M. V. Dolguikh, A. V. Muravjov, and R. E. Peale, *J. Appl. Phys.* 99, 093106 **(2006)**.
20. A. A. Andronov, A. M. Belyantsev, E. P. Dodin, V. I. Gavrilenko, Yu. L. Ivanov, V. A. Kozlov, Z. A. Krasil'nik, L. S. Mazov, A. V. Muravjov, I. M. Nefedov, V. V. Nikanorov, Yu. N. Nozdrin, S. A. Pavlov, V. N. Shastin, V. A. Valov, and Yu. B. Vasil'ev, *Physica B* 134, 210 **(1985)**.
21. Zaubertek, Inc., 1809 E Broadway St. #313, Oviedo, FL 32765, www.zaubertek.com.
22. T. W. Du Bosq, A. V. Muravjov, K. Park, C. Mathis, T. J. Mahaney, M. V. Dolguikh, R. E. Peale, and C. J. Fredricksen, Optical Terahertz Science and Technology Technical Digest, OSA, Washington, DC **(2005)**.
23. H. Weidner and R. E. Peale, *Appl. Spectros.* 51, 1106 **(1997)**.
24. Alpes Lasers SA, 1-3 Max.-de-Meuron, C.P. 1766, CH-2001 Neuchâtel Switzerland.
25. R. Brazis and F. Keilmann, *Solid State Commun.* 70, 1109 **(1989)**.
26. M. V. Dolguikh, A. V. Muravjov, and R. E. Peale, Intravalence-band THz laser in selectively-doped semiconductor structure. *Proc. SPIE* 5365, 184 **(2004)**.
27. M. V. Dolguikh, A. V. Muravjov, R. E. Peale, D. Bliss, C. Lynch, D. W. Weyburne, and W. R. Buchwald, Terahertz gain on inter-valence-band transitions in multilayer delta-doped p-GaAs structures. Terahertz for Military and Security Applications IV, edited by D. L. Woolard, R. J. Hwu, M. J. Rosker, and J. O. Jensen, *Proc. SPIE* 6212, 621206-1 **(2006)**.
28. A. V. Muravjov, M. V. Dolguikh, R. E. Peale, O. A. Kuznetsov, and E. A. Uskova, Amplification of terahertz radiation in delta-doped germanium thin films. Terahertz and Gigahertz Electronics and Photonics IV, edited by R. J. Hwu and K. J. Linden, *Proc. SPIE* 5727, 44 **(2005)**.
29. M. V. Dolguikh, Monte Carlo simulation of hole dynamics and terahertz amplification in multilayer delta doped semiconductor structures. Ph.D. dissertation, University of Central Florida, Orlando **(2005)**.
30. P. Kinsler and W. Th. Wenckebach, *J. Appl. Phys.* 90, 1692 **(2001)**.

Received: 22 August 2006. Revised/Accepted: 2 February 2007.